Inorganic Chemistry

Article

pubs.acs.org/IC

Subtle Changes to Peripheral Ligands Enable High Turnover Numbers for Photocatalytic Hydrogen Generation with Supramolecular Photocatalysts

Tanja Kowacs,[†] Laura O'Reilly,[‡] Qing Pan,[§] Annemarie Huijser,*[,§] Philipp Lang,[†] Sven Rau,[†] Wesley R. Browne,*[,∥] Mary T. Pryce,[‡] and Johannes G. Vos*[,‡]

[†]Institut für Anorganische Chemie I, Universität Ulm, Albert-Einstein-Allee 11, 89081 Ulm, Germany

[‡]SRC for Solar Energy Conversion, School of Chemical Sciences, Dublin City University, Dublin 9, Ireland

[§]Optical Sciences group, MESA + Institute for Nanotechnology, University of Twente, P.O. Box 217, 7500 AE Enschede, The Netherlands

[∥]Stratingh Institute for Chemistry, University of Groningen, Nijenborgh 4, 9747 AG Groningen, The Netherlands

Supporting Information

ABSTRACT: The photocatalytic generation of hydrogen (H_2) from protons by two cyclometalated ruthenium−platinum polypyridyl complexes, $[Ru(bpy)_2(2,5\text{-bpp})PtIS]^{2+}$ (**1**) and $[Ru(dceb)_2(2,5\text{-bpp})PtIS]^{2+}$ (**2**) [where bpy = 2,2′-bipyridine, 2,5-bpp = 2,2′,5′,2″-terpyridine, dceb = 4,4′-di(carboxyethyl)bipyridine, and S = solvent], is reported. Turnover numbers (TONs) for H_2 generation were increased by nearly an order of magnitude by the introduction of carboxyethyl ester units, i.e., from 80 for **1P** to 650 for **2P** after 6 h of irradiation, with an early turnover frequency (TOF) increasing from 15 to 200 h^{-1}. The TON and TOF values for **2P** are among the highest reported to date for supramolecular photocatalysts. The increase correlates with stabilization of the excited states localized on the peripheral ligands of the light-harvesting Ru^{II} center.

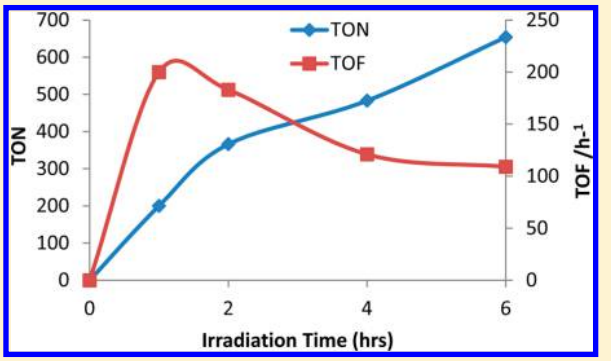

INTRODUCTION

Anthropogenic climate change and an inexorable rise in energy demands are key global challenges, where the hydrogen (H_2) economy is expected to play a key role. Clean, economic, and sustainable approaches to producing H_2 from abundant, renewable energy resources are central to the development of the H_2 economy. A promising method for localized H_2 production is the direct conversion of solar energy to fuel. Intramolecular photocatalytic systems that combine a light-harvesting unit, a bridging ligand, and a catalytic center offer considerable opportunities, and many bimetallic systems have been reported based on combinations such as Ru−Re, Re−Co, Ru−Pt, Os−Rh, Ru−Rh, Pt−Co, and Ir−Rh.[1] In particular, systems where Ru^{II}-based photosensitizers are bound covalently to Pt^{II} or Pd^{II} catalysts have received extensive attention.[2−6] Mononuclear and homodinuclear cyclometalated platinum complexes have been described as catalysts for H_2 generation;[7,8] however, the corresponding heterodinuclear Ru−Pt complexes have yet to be investigated.

Here, we report the first heterodinuclear cyclometalated Ru−Pt systems (**1**/**1P** and **2**/**2P**; Figure 1) capable of photocatalytic H_2 generation in the presence of triethylamine (TEA). The 2,2′,5′,2″-terpyridine (2,5-bpp) bridging ligand enables simultaneous N^N and N^C binding modes for $(bpy)_2Ru^{II}$ type (where bpy = 2,2′-bipyridine) photosensitizers and Pt-based catalytic centers (Figure 1). We show that turnover numbers (TONs) of 650 over 6 h can be achieved with compound **2P**, which, to the best of our knowledge, is the highest catalytic activity achieved to date for dinuclear polypyridyl-based Ru−Pt photocatalysts. Furthermore, we demonstrate that the photocatalytic properties of these assemblies are highly dependent on the nature of the peripheral ligands, i.e., bpy versus 4,4′-di(carboxyethyl)bipyridine (dceb). The data obtained are compared with those reported for the analogous Pd^{II} complex (see Table 1).[9] The paradigm in this field with regard to photocatalyst design is that the bridging ligand should act as an energy/electron reservoir and hence host the lowest-lying excited states. However, it has recently been suggested that this approach may be problematic. If the bridging ligand is to act as a reservoir, transfer of the second electron needed to produce H_2 may be impeded.[10] In addition, recent photophysical studies[11] of compound **5** show that, after photoexcitation, most of the electron density resides on the

Received: August 1, 2015

DOI: 10.1021/acs.inorgchem.5b01752
Inorg. Chem. XXXX, XXX, XXX−XXX

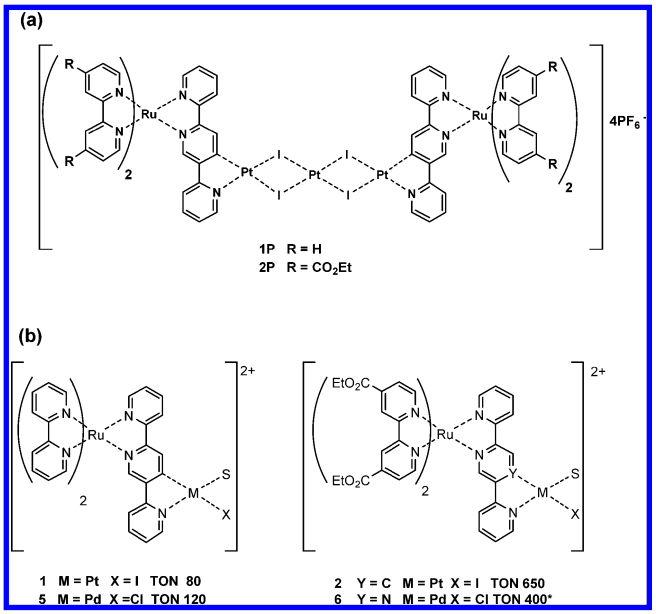

Figure 1. Structures of compounds discussed. (a) Proposed structures of pentanuclear compounds **1P** and **2P** in the solid state. (b) Structures **1** and **2**, formed in situ upon dissolution, and **5** and **6**. Compound **1** was also isolated. TONs after 6 h and (*) 18 h. S = solvent. For photocatalytic conditions, see Figure 4.

Table 1. UV/Vis Absorption and Emission Maxima in Acetonitrile[a]

	absorption λ_{max}/nm (ε/10^4 L/mol·cm)	emission λ_{max}/nm (lifetime/ns, after N_2 purging/%)	TON number after 6 h of irradiation at 470 nm
1/**1P**	460 (1.05)	645 (136, 12; 659, 88)	80*, 99**
2P	483 (1.65)	662 (624)	650**
3	455 (1.18)	632 (790)	69***
4	479 (1.71)	647 (1040)	88***
5[11]	463 (1.33)	635 (88, 38; 400, 62)	120*

[a]Intermolecular and intramolecular photocatalytic studies were performed: (*) dinuclear species; (**) pentanuclear species; (***) intermolecular.

peripheral ligands and that the triplet metal-to-ligand charge-transfer (^{3}MLCT) states involving the bridging ligand lie higher in energy than those of the peripheral ligands. This difference would be expected to limit electronic coupling with the catalytic center and reduce the overall efficiency. However, the dramatic increase in the TON values obtained upon the introduction of 4,4′-di(carboxyethyl) groups on the peripheral ligands would suggest that better matching of the relative energies of the peripheral and bridging ligands improves the catalytic performance of the photocatalysts.

EXPERIMENTAL SECTION

Materials. 4,4′-Di(carboxyethyl)-2,2′-bipyridine,[12] $[Ru(bpy)_2Cl_2]\cdot 2H_2O$,[13] *cis*-$[Pt(DMSO)_2Cl_2]$,[14] and $[Ru(bpy)_2(2,5\text{-bpp})](PF_6)_2$ (**3**)[9] were prepared using literature methods. Solvents obtained were used without further purification.

cis-[Pt(DMSO)$_2$I$_2$] (DMSO = Dimethyl Sulfoxide). *cis*-$[Pt(DMSO)_2Cl_2]$ (1.50 g, 3.6 mmol) and KI (1.50 g, 9.0 mmol) were dissolved in 20 mL of DMSO and stirred for 1.5 h at 50−60 °C. After cooling to room temperature, 100 mL of water (H_2O) was added, and the mixture was allowed to stand at room temperature for 2 h. The orange solid resulting was collected through vacuum filtration, washed with H_2O, ethanol (EtOH), and diethyl ether (Et_2O), and finally dried in vacuo. Yield: 86% (1.85 g, 3.1 mmol). MW: 605.16 g/mol.

cis-[Ru(dceb)$_2$Cl$_2$]·0.5H$_2$O. $RuCl_3\cdot 3H_2O$ (303 mg, 1.16 mmol) was dissolved in 30 mL of EtOH and heated at reflux for 30 min. 4,4′-di(carboxyethyl)-2,2′-bipyridine (696 mg, 2.32 mmol) was added slowly over 45 min, and the reaction mixture was heated at reflux under N_2 for a further 24 h. After cooling, EtOH was removed in vacuo, and the green product was washed with Et_2O and collected by filtration. Yield: 81% (726 mg, 0.94 mmol). ^{1}H NMR (400 MHz, DMSO-d_6): δ 10.11 (d, J = 5.9 Hz, 2H, H-d), 9.14 (d, J = 1.3 Hz, 2H, H-a), 8.95 (d, J = 1.5 Hz, 2H, H-a′), 8.27 (dd, J = 5.9 and 1.7 Hz, 2H, H-c), 7.77 (d, J = 6.1 Hz, 2H, H-d′), 7.49 (dd, J = 6.0 and 1.8 Hz, 2H, H-c′), 4.53 (q, J = 7.0 Hz, 4H, OCH_2), 4.36 (q, J = 7.1 Hz, 4H, OCH_2), 1.45 (t, J = 7.1 Hz, 6H, OCH_2CH_3), 1.31 (t, J = 7.1 Hz, 6H, OCH_2CH_3). Elem anal. Calcd for $C_{32}H_{33}Cl_2N_4O_{8.5}Ru$: C, 49.18; H, 4.22; N, 7.16. Found: C, 49.2; H, 4.2; N, 6.6.

*[Ru(dceb)$_2$(2,5-bpp)](PF$_6$)$_2$·2H$_2$O (**4**·2H$_2$O).* *cis*-$[Ru(dceb)_2Cl_2]\cdot 0.5H_2O$ (487 mg, 0.631 mmol) dissolved in 12 mL of EtOH was added dropwise to a solution of 2,2′:5′,2″-terpyridine (147 mg, 0.631 mmol) in 9 mL of EtOH−H_2O (3:1). The reaction mixture was heated at reflux for 10 h. Subsequently, the mixture was cooled to room temperature, and EtOH was removed in vacuo. The product was precipitated by the addition of aqueous NH_4PF_6, recovered by filtration, and washed with H_2O and Et_2O. The product was recrystallized from acetone−water (3:1). For further purification, the compound was stirred in cold EtOH and filtered repeatedly, affording a brown/reddish solid. Yield: 42% (337 mg 0.263 mmol). MW: 1278.93 g/mol. ^{1}H NMR (400 MHz, acetone): δ 9.41−9.30 (m, 4H, 4*H-a), 8.96 (d, J = 8.3 Hz, 1H, H-3), 8.93 (d, J = 8.0 Hz, 1H, H-3″), 8.86 (dd, J = 8.6 and 1.9 Hz, 1H, H-4), 8.60 (d, J = 1.5 Hz, 1H, H-6), 8.54−8.52 (m, 1H, H-6′), 8.51 (d, J = 5.9 Hz, 1H, H-d), 8.46 (d, J = 5.8 Hz, 1H, H-d), 8.38 (dd, J = 5.6 and 3.1 Hz, 2H, 2H-d), 8.30 (td, J = 8.0, 1.4 Hz, 1H, H-4″), 8.14 (d, J = 5.7 Hz, 1H, H-6″), 8.05−7.94 (m, 4H, 4H-c), 7.90−7.83 (m, 2H, H-4′, H-3′), 7.64−7.58 (m, 1H, H-5″), 7.41 (ddd, J = 6.1, 4.8, and 2.7 Hz, 1H, H-5′), 4.52−4.41 (m, 8H, OCH_2), 1.42−1.34 (m, 12H, OCH_2CH_3). Elem anal. Calcd for $C_{47}H_{47}F_{12}N_7O_{10}P_2Ru$: C, 44.72; H, 3.72; N, 7.77. Found: C, 45.0; H, 3.3; N, 7.5.

*[{Ru(bpy)$_2$(2,5-bpp)PtI$_2$}$_2$Pt](PF$_6$)$_4$·H$_2$O (**1P**·H$_2$O).* *cis*-$[Pt(DMSO)_2I_2]$ (79.5 mg, 0.13 mmol) and **3** (130.6 mg, 0.11 mmol) were dissolved in 30 mL of acetone−EtOH (1:1), and the reaction mixture was heated at reflux for several days until a precipitate formed. After cooling to room temperature, a precipitate was isolated by filtration and attributed to the pentanuclear structure. Elem anal. Calcd for $C_{70}H_{54}F_{24}I_4N_{14}OP_4Pt_3Ru_2$: C, 28.40; H, 1.81; N, 6.57. Found: C, 28.36; H, 1.77; N, 6.62. ICP. Calcd: Pt, 19.62; Ru, 6.77. Found: Pt, 17.74; Ru, 6.13. Subsequently, this solid was dissolved in acetonitrile (the use of a coordinating solvent breaks up the pentanuclear structure formed initially), followed by filtration and removal of the solvent in vacuo. The residue was dissolved in the minimum of H_2O and precipitated in an aqueous solution of NH_4PF_6, followed by filtration. The brown solid was then washed with H_2O and the minimum of EtOH and Et_2O to yield 137 mg (0.103 mmol) of the dinuclear species. Overall yield: 93%.

*[Ru(bpy)$_2$(2,5-bpp)PtI(H$_2$O)](PF$_6$)$_2$·3H$_2$O (**1**.* ^{1}H NMR (400 MHz, DMSO-d_6): δ 10.19 (d, J = 5.8 Hz, 1H, H-6′), 9.61 (s, 1H, H-3), 8.82 (t, J = 8.2 Hz, 4H, H-a), 8.33 (d, J = 8.2 Hz, 1H, H-3″), 8.27−8.11 (m, 6H, H-4′, H-4″, 4H-b), 7.96 (d, J = 4.8 Hz, 1H, H-d), 7.81 (d, J = 4.7 Hz, 1H, H-d), 7.78 (s, 1H, H-6), 7.76−7.67 (m, 3H, H-6″, 2H-d), 7.63 (t, J = 7.4 Hz, 1H, H-5′), 7.60−7.49 (m, 5H, H-5″, 4′H-c), 7.46 (d, J = 8.3 Hz, 1H, H-3′). Elem anal. Calcd for $C_{35}H_{34}N_7F_{12}IO_4P_2PtRu$: C, 31.61; H, 2.58; N, 7.37. Found: C, 31.4; H, 2.1; N, 6.9.

*[{Ru(dceb)$_2$(2,5-bpp)PtI$_2$}$_2$Pt](PF$_6$)$_4$ (**2P**).* *cis*-$[Pt(DMSO)_2I_2]$ (74.9 mg, 0.123 mmol) and **4**·2H$_2$O (123.0 mg, 0.096 mmol) were dissolved in 30 mL of acetone−EtOH (1:1), and the reaction mixture was heated at reflux for 7 days. After cooling to room temperature, the product was precipitated in an aqueous solution of NH_4PF_6, followed

DOI: 10.1021/acs.inorgchem.5b01752
Inorg. Chem. XXXX, XXX, XXX−XXX

by filtration. The red solid was then washed with H_2O and Et_2O. Yield (based on the formation of a pentanuclear structure): 90% (136 mg, 0.087 mmol). ^{1}H NMR (400 MHz, DMSO-d_6): δ 9.75 (d, J = 5.4 Hz, 1H, H-6′), 9.20 (s, 1H, H-3), 8.80−8.92 (m, 4H, 4H-a), 7.92 (d, J = 8.2 Hz, 1H, H3″), 7.81 (t, J = 8.4 Hz, 1H, H-4″), 7.74 (d, J = 5.8 Hz, 2H, H-d, H-4′), 7.57 (t, J = 6.9 Hz, 1H, H-d), 7.45−7.55 (m, 4H, H-6, H-d, 2H-c), 7.35−7.42 (m, 3H, 2H-c, H-d), 7.28 (d, J = 5.6 Hz, 1H, H-6″), 7.17 (d, J = 8.3 Hz, 2H, H-5′, H-3′), 7.11−7.03 (m, 1H, H.5″), 3.95−4.05 (m, 8H, OCH_2), 0.95−0.87 (m, 12H, OCH_2CH_3). Elem anal. Calcd for pentanuclear structure $C_{94}H_{84}F_{24}I_4N_{14}O_{16}P_4Pt_3Ru_2$: C, 31.89; H, 2.39; N, 5.4. Found: C, 31.88; H, 2.17; N, 5.45. Compound **2** is obtained in situ upon dissolution in acetonitrile.

^{1}H NMR spectra were obtained on a Bruker Advance 400 NMR spectrometer in acetone-d_6, acetonitrile-d_3, or DMSO-d_6 with either trimethylsilane (TMS) or residual solvent peaks as the reference. Free induction decay profiles were processed using a MestReNova. Spin multiplicities are indicated with the abbreviations s (singlet), d (doublet), t (triplet), q (quartet), dd (doublet of a doublet), and m (multiplet) and coupling constants, J, in hertz. CHN analyses were carried out using an Exador Analytical CE440 analyzer by the Microanalytical Department, University College Dublin. Elemental analyses for Ru and Pt were recorded using a Optima 8300 inductively coupled plasma atomic emission spectroscopy (ICP-OES) system with high-temperature sample destruction by microwave digestion in concentrated HNO_3 and carried out by the Chemical Analysis Service center at the University of Groningen. Electrospray ionization mass spectrometry spectra in acetonitrile were recorded in positive mode on a Triple Quadrupole liquid chromatography (LC)/MS/MS spectrometer (API 3000, PerkinElmer Sciex Instruments). UV/vis absorption spectra were recorded on an Agilent Technologies 8453 photodiode array spectrometer using a 1-cm-path-length quartz cell. Emission spectra (accuracy ±5 nm) were obtained using a LS50B luminescence spectrophotometer, equipped with a red-sensitive Hamamatsu R928 PMT detector, interfaced with an Elonex PC466 employing PerkinElmer FL WinLab, with an optical density of ca. 0.2 for all solutions at the wavelength of excitation.

Resonance Raman (rR) spectra were recorded at 473 nm (100 mW), 457 nm (45 mW), and 355 nm (10 mW) (Cobolt Lasers) in 1-cm-path-length quartz cuvettes. The excitation beam was focused at the sample using a 10-cm-focal-length parabolic mirror at ca. 35° with respect to the collection axis. The Raman scattering was collected and collimated with a 2.5-cm-diameter, 15-mm-focal-length plano convex mirror, filtered to remove Rayleigh scattering using a Steep Edge long-pass filter (Semrock), focused into the spectrograph (Shamrock 303, AndorTechnology, 1200 mm^{-1} grating blazed at 500 nm), and imaged onto an Andor iDus-420-BEX2-DD CCD camera.

Time-resolved photoluminescence (PL) decays were recorded using a FluoroMax spectrofluorometer extended for time-correlated single-photon-counting measurements (Horiba Jobin Yvon, Fluoro-Max-4 TCSPC). A NanoLED-460 laser source (462 nm, 1.3 ns pulse duration) was used to excite the samples at repetition rates of 100 kHz for **1P**, **2P**, and **3** and 50 kHz for **4**. Samples were dissolved in acetonitrile and degassed using dry N_2 gas for 20 min before the PL measurements.

Wavelength-dependent measurements were performed in a "back and forth" sequence: λ_{max} (the wavelength of maximum PL intensity), 680, 640, 720, 600, and 760 nm, and finally λ_{max} again. The occurrence of oxygen leakage was excluded by comparing the final measurement at λ_{max} with the first measurement. The fits were performed with fixed offset values based on the average number of dark counts.

Photocatalytic Experiments. All solutions used were degassed prior to irradiation. In order to produce a stock solution, an exact sample weight was dissolved in 20 mL of acetonitrile. The sample solution of the complexes in the gas chromatography (GC) vials was then prepared by mixing 1.2 mL of the stock solution, 0.2 mL of H_2O (10%), and 0.6 mL of TEA under a N_2 atmosphere. The sample solutions contained 1.17 × 10^{-4} mol/L photocatalyst. For the experiments, the sample solutions (2 mL) were filled in GC vials, which were irradiated for several hours at 470 nm using light-emitting diodes (LEDs, 40−50 mW). The irradiation occurs from below, and the vials are cooled by cooling fans from the side, in order to keep the catalytic solutions at room temperature. After irradiation, the amount of H_2 produced was measured by means of GC after 0, 1, 2, 4, 6, 18, and 24 h and an average of three samples was taken for calculating the TON and TOF values. H_2 evolution was determined by headspace GC using a Bruker Scion gas chromatograph/mass spectrometer, with thermal conductivity detection (column, molecular sieve 5A, 75 m × 0.53 mm i.d.; oven temperature 70 °C; flow rate 22.5 mL/min; detector temperature 200 °C) with argon as the carrier gas.·

RESULTS AND DISCUSSION

The ligand 2,5-bpp and the precursors **3** and **4** were prepared using literature methods as described in the experimental part. Ru^{II}−Pt^{II} complexes **1** and **2** were obtained by the reaction of **3** and **4** with *cis*-$[Pt(DMSO)_2I_2]$. Both RuPt compounds were isolated as solids from the reaction mixture after several days of reflux. Surprisingly, elemental analysis and ICP indicated that, in the solid state the products obtained, **1P** and **2P** are pentanuclear compounds, as shown in Figure 1a, with a Ru−Pt−Pt−Pt−Ru moiety bridged by iodide ligands. Such PtI arrangements are not unusual, and some X-ray structures have been reported.[15] However, these PtI assemblies tend to decompose in the presence of coordinated ligands such as acetonitrile. This was indeed observed when **1P** and **2P** were dissolved in acetonitrile prior to obtaining mass (see Table S1 and Figure S1) and ^{1}HNMR spectra for numbering of protons (see Figures S2−S7). These techniques indicate only the presence of dinuclear species with the overall formula $[Ru(N\text{^}N)_2(2,5\text{-bpp})PtI(S)](PF_6)$, where S = solvent, and signals indicative of pentanuclear compounds are not observed. This suggests that, upon dissolution of the pentanuclear complexes, dinuclear species with the structure $[Ru(N\text{^}N)_2(2,5\text{-bpp})PtI(S)]^{2+}$ are formed as shown in Figure 1 and are in agreement with the structure observed for compound **5**.[9]

The most notable change in the ^{1}H NMR spectra upon cyclometalation of **3** and **4** with the Pt catalyst is a shift downfield of the two signals assigned to H6′ and H3 of the 2,5-bpp ligand due to deshielding by Pt^{II} (see Figures S5 and S6). ^{1}H NMR spectra of **2P** confirm that ester hydrolysis does not occur during synthesis and purification.

Importantly, because in acetonitrile the penta- and dinuclear species show the same ^{1}H NMR spectra, this indicates that in that solvent the pentanuclear species releases a Pt center and that two dinuclear RuPt compounds are formed. In the manuscript, **1** and **2** therefore describe the dinuclear compounds $[Ru(bpy)_2(2,5\text{-bpp})PtI(CH_3CN)]^{2+}$ and $[Ru(dceb)_2(2,5\text{-bpp})PtI(CH_3CN)]^{2+}$ (see Figure 1b), respectively. For most measurements, pentanuclear samples were used, and therefore the labels **1P** and **2P** are used in the text to identify the compounds studied, but it should be kept in mind that the species present in solution and active in the photocatalytic studies are **1** and **2**, respectively.

The nature of the Pt species released at this disproportionation is at present unclear, but in acetonitrile, the formation of a species such as *cis*-$[Pt(CH_3CN)_2I_2]$ is most likely. The potential effect of this species on the photocatalytic effect is discussed below.

The UV/vis absorption and emission spectra of **1P**, **2P**, **3**, and **4** (Figure 2 and Table 1) are typical of ruthenium(II) polypyridyl complexes. The transitions in the UV spectra are assigned to π−π^* transitions of the polypyridyl ligands, with the band at 330−370 nm assigned to the 2,5-bpp ligand and the

DOI: 10.1021/acs.inorgchem.5b01752
Inorg. Chem. XXXX, XXX, XXX−XXX

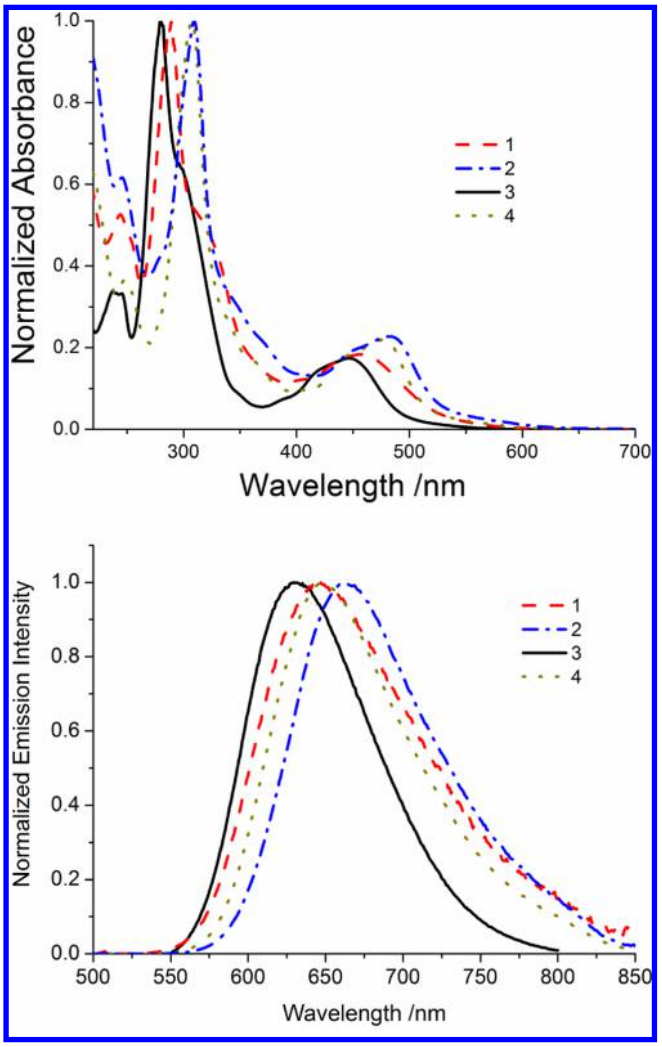

Figure 2. UV/vis absorption and emission (λ_{exc} = 450 nm) spectra of **1**–**4** in acetonitrile.

transitions at λ > 350 nm to singlet-state MLCT (^{1}MLCT) transitions (vide infra).[16] The bathochromic shift of the π–π^* transitions at 300 nm upon the introduction of ester moieties (i.e., in **2P** and **4**) reflects the stabilization provided by these electron-withdrawing moieties. The visible absorption spectra of **1P** and **2P** are generally similar to those of the mononuclear complexes **3** and **4**, respectively, indicating that orthometalation by Pt^{II} has a minor influence on the electronic structure of the Ru^{II} moiety. Complexation to Pt^{II} results in ca. a 15 nm bathochromic shift in the emission maxima and a decrease in the emission decay lifetimes in both cases. The absorption and emission data (Figure 2) show that the changes in the shape and position of the ^{1}MLCT absorption bands upon the introduction of ester moieties are relatively minor and that there is little change in the molar absorptivities of **1P** and **2P** at the wavelength of irradiation for photocatalysis (470 nm). Therefore, the improved photocatalytic efficiency is not related to the increased molar absorptivity in the case of **2P**. Although, **2P**, **3**, and **4** show wavelength-independent monoexponential emission decay kinetics (Table 1), **1P** decays biexponentially (136 and 659 ns), albeit with no wavelength dependence (Table S2), as previously observed for the analogous Ru–Pd complex **5** ($[Ru(bpy)_2(2,5\text{-bpp})PdClCH_3CN]^{2+}$),[9] for which the faster process was assigned to relaxation from a 2,5-bpp-ligand-localized ^{3}MLCT state. The monoexponential decay observed for **2P** indicates that its excited-state dynamics differ from those of **1P**.

rR spectra of **1**/**1P**, **2P**, and **4** were recorded at λ_{exc} = 355 nm (Figure S8), 457 nm (Figure S9), and 473 nm (Figure 3).

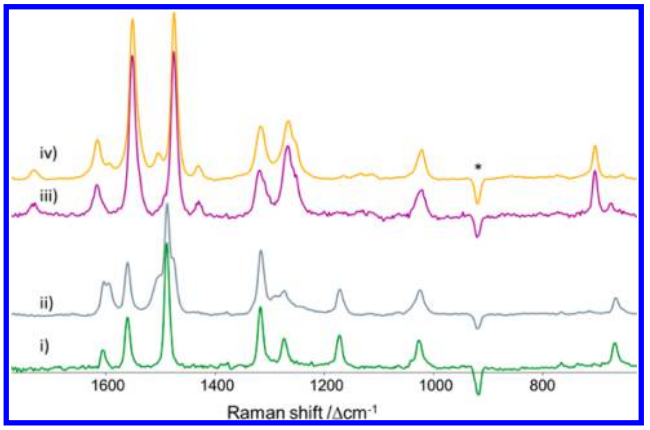

Figure 3. rR spectra at λ_{exc} = 473 nm of (i) $[Ru(bpy)_3]^{2+}$, (ii) **1P**, (iii) **4**, and (iv) **2P** in acetonitrile with subtraction of the solvent contributions. The asterisk indicates a peak due to imperfect solvent subtraction.

Resonance enhancement of Raman scattering is observed only for modes of the chromophoric moiety, which facilitates assignment of the ^{1}MLCT and π–π^* absorption bands (see Table 1 for major bands).[17] The spectra of **3**[9,11] and **4** are almost identical with that of $[Ru(bpy)_3]^{2+}$ except for shoulders on either side of the band at 1489 cm^{-1} and an increase in the relative intensity of the band at 1606 cm^{-1} indicating that 2,5-bpp-based ^{1}MLCT absorption bands, in addition to bpy-based ^{1}MLCT transitions, are present. In the case of **4**, additional bands related to the ester moiety are observed also. Hence, the transitions at 473 nm are assigned primarily but not exclusively to ^{1}MLCT (π_{bpy}^* ← t_2) transitions.[11] For **1**/**1P** and **2P**, additional bands are observed at 1290, 1476, 1504, 1594, and 1606 cm^{-1}, as observed earlier for the related Pd^{II} analogue **5**,[11] indicating that excitation at 473 nm is resonant with ^{1}MLCT ($\pi_{2,5\text{-bpp}}^*$ ← t_2) transitions also. Hence, rR spectroscopy indicates that excitation at 457 and 473 nm leads to the initial population of both bpy- and bridging-ligand-based ^{1}MLCT states for **1P** to **4**, albeit with varying relative contributions and with a decrease, compared with **1P**, in the contributions from the bridging ligand on the long-wavelength side of the spectrum of **2P**. Raman spectroscopy at λ_{exc} = 355 nm shows enhancement of primarily 2,5-bpp features for both the mono- and heterobimetallic complexes (Figure S8), with a substantial change observed upon coordination of Pt^{II}, as expected.

Photocatalytic studies were performed on the isolated pentamer and penta/dinuclear assemblies, in addition to intermolecular photolysis using compounds **3** and **4** together with *cis*-$[Pt(CH_3CN)_2I_2]$. The H_2 generation capacity of **1**, **1P**, and **2P** was studied for up to 18 h of irradiation in triplicate. Typical examples of H_2 gas generation over the first 6 h are shown in Figure 4 (Table 1; see the figure legend for the experimental conditions). The photocatalytic activity of compound **1P**, with a TON of 99 after 6 h (100 after 18 h), is similar to that observed for **5**[9] (Figure 4) and indicates that for the bpy analogue the replacement of a Pd center with the

DOI: 10.1021/acs.inorgchem.5b01752
Inorg. Chem. XXXX, XXX, XXX–XXX

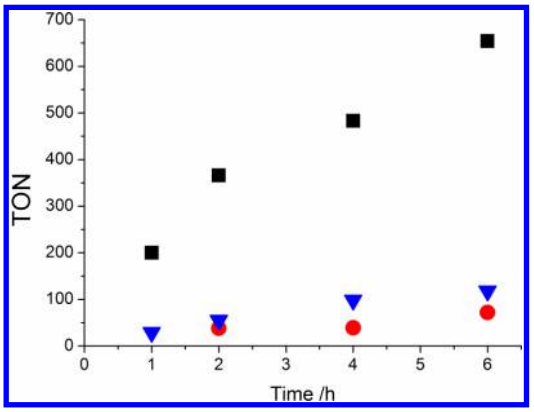

Figure 4. TON values for **1P** (red), **2P** (black), and **5** (blue)[9] [1.17×10^{-4} mol/L in 6:3:1 (v/v/v) CH_3CN–TEA–H_2O; under continuous irradiation at 470 nm].

Pt-based catalytic center does not improve the catalytic behavior. However, the introduction of carboxyethyl moieties on the peripheral ligands of **2P** results in almost an order of magnitude increase in activity to 650 after 6 h (720 over 18 h). In addition, TOFs of up to 200 h^{-1} are observed in the early stage of the catalytic reaction. A number of control experiments were also carried out. Irradiation of compounds **3**, **4**, *cis*-$[Pt(CH_3CN)_2I_2]$, or TEA individually using the same experimental conditions did not produce H_2. Upon irradiation of equimolar mixtures of the photosensitizer and the catalytic center using *cis*-$[Pt(CH_3CN)_2I_2]$ as the catalyst, TON values of 69 and 88 were obtained for compounds **3** and **4**, respectively, after 6 h (see Table 1). During these intermolecular experiments, colloid formation was observed. In the preformed heterobimetallic complexes, a small quantity of colloid formation was observed for the pentanuclear complex **1P**.

As shown in the experimental part, both the pentanuclear (**1P**) and dinuclear (**1**) forms were isolated. The latter was obtained by dissolving the pentanuclear compound in acetonitrile. The dinuclear species (**1P**) shows CHN analysis and ^1H NMR spectroscopic data that are in agreement with those of $[Ru(bpy)_2(2,5\text{-bpp})PtI(S)](PF_6)_2$, i.e., a monoplatinum complex.

Photocatalytic studies for both **1P** and **1** were carried out to estimate any potential effect that the "free Pt" generated in situ may have on photocatalysis. The data obtained show that, for the pentanuclear precursor complex, a TON of 99 is obtained, while for the dinuclear analogue, a value of 80 is obtained. As outlined above, intermolecular studies using equimolar amounts of the precursor **3** and *cis*-$[Pt(CH_3CN)_2I_2]$ show TONs of 69. Hence, the mononuclear Pt species released upon dissolution of **1P** does not appear to contribute significantly to H_2 generation.

The influence of the ester groups on the photocatalytic H_2 generation capacity of the supramolecular assemblies presented here are consistent with the findings reported for the related complexes $[Ru(bpy)_2(2,5\text{-dpp})PdCl_2]^{2+}$ [where 2,5-dpp = 2,5-bis(pyrid-2-yl)pyrazine], which did not produce H_2 and $[Ru(dceb)_2(2,5\text{-dpp})PdCl_2]^{2+}$ (**6**; see Figure 1b), which showed a TON value of 400 after 18 h. Hence, H_2 generation increases considerably by the introduction of ester moieties on the peripheral ligands.[6a] The results show that, apart from manipulation of the bridging ligands[1b,9] and the catalytic center,[18] changes in the peripheral ligands can also greatly improve the photocatalytic efficiency of photocatalysts. UV/vis absorption and emission spectroscopy indicate that the introduction of the carboxyethyl substituent lowers the energy of the MLCT states located on the peripheral ligand, and hence one could anticipate that this would decrease the catalytic activity because this energy may now be lower than that of the bridging ligand. However, the opposite is observed. The exact cause of the 7-fold increase (after 18 h) in TON upon the introduction of the ester groups is at present unclear. Spectroscopic data as well as emission lifetime studies suggest that **1P** and **2P** have distinctly different photophysical properties, and the study of these properties will be the focus of future efforts.

CONCLUSION

In the wider field of photocatalytic solar fuel production by supramolecular assemblies, the best approach to optimization of the interaction between the photosensitizer and catalytic center with regard to the overall photocatalytic activity is still a matter of debate. At present, for assemblies designed for H_2 generation, bridging ligands that allow for weak-to-medium interaction between these two components have emerged as the most active.[1] However, in the area of CO_2 reduction, the use of bridging ligands that provide little or no through-bond interaction between the photosensitizer and catalytic center appears to be the better approach.[19] This difference reflects the complexity of the overall two-electron reduction processes and highlights the experimental challenge faced in disentangling the several distinct elementary steps that the overall reactions involve. Unfortunately, detailed kinetic studies on supramolecular assemblies of this type are at present not available. More detailed photophysical studies are needed to allow for a detailed discussion on what processes are dominant, ranging from coupling between the various orbitals to the influence of a possible back-reaction. Also the issue of reductive versus oxidative quenching needs to be considered. In the design of photocatalytic assemblies for H_2 generation, considerable attention has been devoted to the choice of the various components present in the supramolecular systems, such as the bridging ligand, the catalytic center, and the nature of the photosensitizer. Efforts have been directed toward balancing the overall efficiency of photoinduced intramolecular electron transfer between the light-harvesting unit and catalytic center and in maintaining a sufficiently long-lived excited state to allow for reduction of the light-harvesting unit by the terminal reductant.

In this contribution, a significant improvement in the efficiency of light-driven H_2 generation by intramolecular photocatalysts is reported in terms of both TON and TOF, which are, to the best of our knowledge, among the highest catalytic activities reported for intramolecular Ru-based supramolecular assemblies. Most importantly, it is shown here that the peripheral ligands of the light-harvesting unit can have as dramatic an influence on the catalytic efficiency as the bridging unit or catalytic center and that further studies are needed in this area.

ASSOCIATED CONTENT

Supporting Information

The Supporting Information is available free of charge on the ACS Publications website at DOI: 10.1021/acs.inorgchem.5b01752.

Additional ^1H NMR, PL, and MS data (PDF)

DOI: 10.1021/acs.inorgchem.5b01752
Inorg. Chem. XXXX, XXX, XXX–XXX

AUTHOR INFORMATION

Corresponding Authors

*E-mail: j.m.huijser@utwente.nl. Tel: ++35317005307.
*E-mail: w.r.browne@rug.nl.
*E-mail: han.vos@dcu.ie.

Notes

The authors declare no competing financial interest.

ACKNOWLEDGMENTS

The authors thankful for the COST Action PERSPECT H2O CM1202 for support (STSM Nos. 16737 and 150615-060208). Financial support comes from the European Research Council (Grant ERC-2011-StG-279549 to W.R.B.), Science Foundation Ireland (Grants SFI/TIDA/E2763 and SFI/TIDA/2435 MTP), and The Netherlands Ministry of Education, Culture and Science (Gravity Program 024.001.035 to W.R.B.). Dr. A. Serpe of the University of Calabria is thanked for discussion.

REFERENCES

(1) (a) Rau, S.; Walther, D.; Vos, J. G. *Dalton Trans.* **2007**, *18*, 915. (b) Schulz, M.; Karnahl, M.; Schwalbe, M.; Vos, J. G. *Coord. Chem. Rev.* **2012**, *256*, 1682. (c) Frischmann, P. D.; Mahata, K.; Wurthner, F. *Chem. Soc. Rev.* **2013**, *42*, 1847. (d) Manbeck, G. F.; Brewer, K. J. *Coord. Chem. Rev.* **2013**, *257*, 1660. (e) Halpin, Y.; Pryce, M. T.; Rau, S.; Dini, D.; Vos, J. G. *Dalton Trans.* **2013**, *42*, 16243. (f) Artero, V.; Chavarot-Kerlidou, M.; Fontecave, M. *Angew. Chem., Int. Ed.* **2011**, *50*, 7238. (g) Gholamkhass, B.; Mametsuka, H.; Koike, K.; Tanabe, T.; Furue, M.; Ishitani, O. *Inorg. Chem.* **2005**, *44*, 2326.

(2) (a) Rau, S.; Schäfer, B.; Gleich, D.; Anders, E.; Rudolph, M.; Friedrich, M.; Görls, H.; Henry, W.; Vos, J. G. *Angew. Chem., Int. Ed.* **2006**, *45*, 6215. (b) Karnahl, M.; Kuhnt, C.; Ma, F.; Yartsev, A.; Schmitt, M.; Dietzek, B.; Rau, S.; Popp, J. *ChemPhysChem* **2011**, *12*, 2101. (c) Pfeffer, M. G.; Schäfer, B.; Smolentsev, G.; Uhlig, J.; Nazarenko, E.; Guthmuller, J.; Kuhnt, C.; Wächtler, M.; Dietzek, B.; Sundström, V.; Rau, S. *Angew. Chem., Int. Ed.* **2015**, *54*, 5044.

(3) (a) Ozawa, H.; Haga, M.; Sakai, K. *J. Am. Chem. Soc.* **2006**, *128*, 4926. (b) Ozawa, H.; Yokoyama, Y.; Haga, M.; Sakai, K. *Dalton Trans.* **2007**, *12*, 1197. (c) Ozawa, H.; Sakai, K. *Chem. Commun.* **2011**, *47*, 2227.

(4) (a) Suneesh, C. V.; Balan, B.; Ozawa, H.; Nakamura, Y.; Katayama, T.; Muramatsu, M.; Nagasawa, Y.; Miyasaka, H.; Sakai, K. *Phys. Chem. Chem. Phys.* **2014**, *16*, 1607. (b) Sakai, K.; Ozawa, H. *Coord. Chem. Rev.* **2007**, *251*, 2753.

(5) Yam, V. W. W.; Lee, V. W.W.; Cheung, K. K. *J. Chem. Soc., Chem. Commun.* **1994**, *18*, 2075.

(6) (a) Singh Bindra, G.; Schulz, M.; Paul, A.; Soman, S.; Groarke, R.; Inglis, J.; Pryce, M. T.; Browne, W. R.; Rau, S.; Maclean, B. J.; Vos, J. G. *Dalton Trans* **2011**, *40*, 10812. (b) Lei, P.; Hedlund, M.; Lomoth, R.; Rensmo, H.; Johansson, O.; Hammarström, L. *J. Am. Chem. Soc.* **2008**, *130*, 26.

(7) (a) Brooks, J.; Babayan, Y.; Lamansky, S.; Djurovich, P. I.; Tsyba, I.; Bau, R.; Thompson, M. E. *Inorg. Chem.* **2002**, *41*, 3055. (b) Karakus, C.; Fischer, L. H.; Schmeding, S.; Hummel, J.; Risch, N.; Schäferling, M.; Holder, E. *Dalton Trans.* **2012**, *41*, 9623. (c) Ma, D.-L.; Che, C.-M.; Yan, S.-C. *J. Am. Chem. Soc.* **2009**, *131*, 1835. (d) Zucca, A.; Petretto, G. L.; Stoccoro, S.; Cinellu, M. A.; Manassero, M.; Manassero, C.; Minghetti, G. *Organometallics* **2009**, *28*, 2150. (e) Kvam, P.-I.; Puzyk, M. V.; Balashev, K. P.; Songstad, J.; Lundberg, C.; Arnarp, J.; Björk, L.; Gawinecki, R. *Acta Chem. Scand.* **1995**, *49*, 335. (f) Depriest, J.; Zheng, G. Y.; Goswami, N.; Eichhorn, D. M.; Woods, C.; Rillema, D. R. *Inorg. Chem.* **2000**, *39*, 1955.

(8) (a) Deuschel-Cornioley, C.; Luond, R.; von Zelewsky, A. *Helv. Chim. Acta* **1989**, *72*, 377. (b) Jolliet, P.; Gianini, M.; von Zelewsky, A.; Bernardinelli, G.; Stoeckli-Evans, H. *Inorg. Chem.* **1996**, *35*, 4883. (c) Mdleleni, M. M.; Bridgewater, J. S.; Watts, R. J.; Ford, P. C. *Inorg. Chem.* **1995**, *34*, 2334. (d) Kobayashi, M.; Masaoka, S.; Sakai, K. *Photochem. Photobiol. Sci.* **2009**, *8*, 196. (e) Kobayashi, M.; Masaoka, S.; Sakai, K. *Molecules* **2010**, *15*, 4908.

(9) Singh Bindra, G.; Schulz, M.; Paul, A.; Groarke, R.; Soman, S.; Inglis, J. L.; Browne, W. R.; Pfeffer, M.; Rau, S.; MacLean, B. J.; Pryce, M. T.; Vos, J. G. *Dalton Trans* **2012**, *41*, 13050−13059.

(10) Zedler, L.; Guthmuller, J.; Rabelo de Moraes, I.; Kupfer, S.; Krieck, S.; Schmitt, M.; Popp, J.; Rau, S.; Dietzek, B. *Chem. Commun.* **2014**, *50*, 5227.

(11) Pan, Q.; Mecozzi, F.; Korterik, J. P.; Sharma, D.; Herek, J. L.; Vos, J. G.; Browne, W. R.; Huijser, A. *J. Phys. Chem. C* **2014**, *118*, 20799.

(12) Oki, A. R.; Morgan, R. J. *Synth. Commun.* **1995**, *25*, 4093.

(13) Sullivan, B. P.; Salmon, D. J.; Meyer, T. J. *Inorg. Chem.* **1978**, *17*, 3334.

(14) Fang, Y. Q.; Hanan, G. S. *Synlett* **2003**, *6*, 852.

(15) (a) Rogers, R. D.; Isci, H.; Mason, W. R. *J. Crystallogr. Spectrosc. Res.* **1984**, *14*, 383. (b) Martin-Gil, J.; Martin-Gil, F. J.; Pérez-Méndez, M.; Fayos, J. *Z. Kristallogr.* **1985**, *173*, 179. (c) Fanizzi, F. P.; Intini, F. P.; Maresca, L.; Natile, G.; Pacifico, C. *Acta Crystallogr., Sect. C: Cryst. Struct. Commun.* **1999**, *55*, 712.

(16) Juris, A.; Balzani, V.; Barigelletti, F.; Campagna, S.; Belser, P.; von Zelewsky, A. *Coord. Chem. Rev.* **1988**, *84*, 85.

(17) (a) McClanahan, S. F.; Dallinger, R. F.; Holler, F. J.; Kincaid, J. R. *J. Am. Chem. Soc.* **1985**, *107*, 4853. (b) Danzer, G. D.; Golus, J. A.; Kincaid, J. R. *J. Am. Chem. Soc.* **1993**, *115*, 8643. (c) Sykora, M.; Kincaid, J. R. *Inorg. Chem.* **1995**, *34*, 5852.

(18) Pfeffer, M. G.; Kowacs, T.; Wächtler, M.; Guthmuller, J.; Dietzek, B.; Vos, J. G.; Rau, S. *Angew. Chem., Int. Ed.* **2015**, *54*, 6627.

(19) (a) Windle, C. D.; George, M. W.; Perutz, R. N.; Summers, P. A.; Sun, X. Z.; Whitwood, A. C. *Chem. Sci.* **2015**, *6*, 6847. (b) Takeda, H.; Ishitani, O. I. *Coord. Chem. Rev.* **2010**, *254*, 346.

DOI: 10.1021/acs.inorgchem.5b01752
Inorg. Chem. XXXX, XXX, XXX−XXX